Catalysis Science & Technology

ROYAL SOCIETY OF CHEMISTRY

PAPER

View Article Online
View Journal | View Issue

Cite this: *Catal. Sci. Technol.*, 2025, **15**, 1055

Unravelling the deactivation of CuZnO-based catalysts at the industrial scale: a micro to macro scale perspective†

Vera P. Santos, *[a] Ewa Tocha,[b] Jin Yang,[c] Mark McAdon,[a] Carla Schmidt,[c] Stuart Leadley,[d] David Yancey,[a] Stefan van Bloois,[b] Joost Depicker,[b] Swati Naik,[a] Linh Bui,[e] Saurabh Bhandari,[e] Daniel Grohol[a] and David G. Barton[a]

Unexpected changes in catalyst performance can have a significant impact on manufacturing plant operations with respect to both economics and sustainability. The useful lifespan of a catalyst is influenced by various factors, including catalyst performance aging (activity and selectivity), or the mechanical damage of catalyst pellets leading to high reactor pressure drops. Deactivation of industrial catalysts often results from thermal (metal sintering, loss of active surface areas, and vaporization), chemical (poisons: inorganic and organic and fouling), and mechanical mechanisms (abrasion, fracture, and dusting). Conducting a proper root-cause analysis can be complex and typically requires multidimensional fundamental scientific approaches. This study illustrates the mechanical degradation of CuZnO catalyst pellets under industrial hydrogenation conditions, leading to an increased pressure drop and reduced catalyst lifetime. Post-mortem analysis at different length scales in combination with the development of accelerating aging tools played a substantial role in the identification of catalyst failure modes for these industrial catalysts. Careful interpretation of the microscopy results enabled the identification of characteristic fingerprints of the failure mechanism. The presence of organic chloride impurities in the feed in combination with a reducing atmosphere accelerated both the sintering of ZnO and deformation of the catalyst pills. This reduced the effective lifespan of the catalyst, as the decrease in particle void fractions led to an increased reactor pressure drop, eventually necessitating the reloading of the reactor with a fresh catalyst. Understanding these mechanisms at both micro and macro scales is crucial for improving the economics and sustainability of commercial operations.

Received 31st October 2024,
Accepted 3rd January 2025

DOI: 10.1039/d4cy01323a

rsc.li/catalysis

Introduction

Catalysis plays a crucial role in the chemical industry by significantly improving the process efficiency through the acceleration of desired reactions.[1,2] Designing a catalyst for an industrial process is typically a lengthy and complex task, shaped by the nature of the chemical reaction, scale, and operating conditions. Important criteria in catalyst design that must be balanced encompass intrinsic activity, selectivity, stability, and operational robustness. The selection of a catalyst that functions optimally within the given process constraints is extremely valuable, as it has direct implications for the efficiency and carbon footprint of the overall process.[2] Catalyst deactivation is, however, unavoidable and can occur over varying time scales, depending on factors such as the feed composition, production rate, temperature, chemistry, impurities in the feed, and/or sudden changes in operation.[1,3] The catalyst lifetime can range from seconds to years, which has significant implications for process design. Consequently, lifetime is one of the critical metrics in selecting an industrial catalyst, yet it remains one of the most challenging to quantify or predict, often being addressed in the later stages of catalyst development.

At an industrial scale, catalyst deactivation is a complex, multi-dimensional issue, often involving multiple confounding mechanisms, and manifesting itself in different ways, such as loss of activity, selectivity, and/or loss of mechanical strength. Loss of mechanical strength leads to a high pressure drop, which requires an increase in the inlet pressure to maintain the flow through the reactor. This is highly undesirable and eventually causes plant shutdowns. Minimizing pressure drops is crucial for maintaining high

[a] *Core R&D, The Dow Chemical Company, 633 Washington Street, Midland, MI 48667, USA. E-mail: santos.verapatricia@icloud.com*
[b] *Core R&D, Dow Benelux, Herbert Dowweg, Hoek, The Netherlands*
[c] *Tech Center, The Dow Chemical Company, Lake Jackson, Texas 77566, USA*
[d] *Core R&D, Dow Silicones Belgium, Seneffe, Belgium*
[e] *Core R&D, The Dow Chemical Company, Lake Jackson, Texas 77566, USA*
† Electronic supplementary information (ESI) available. See DOI: https://doi.org/10.1039/d4cy01323a

productivity, energy efficiency, and catalyst longevity in hydrogenation reactors. Consequently, identifying the true cause of catalyst deactivation can be challenging due to the presence of various root causes. An integrated approach is generally applied to understand the deactivation mechanism, wherein the active phase is analysed using multiple catalyst characterization tools, and the properties of fresh and spent catalysts are correlated with process operating conditions. Additionally, to test a hypothesized deactivation mechanism, accelerated aging protocols are developed to replicate the failure modes observed in the industrial reactor.[4]

In the literature, catalyst deactivation of heterogeneous catalysts is generally categorized into several types, including: (1) poisoning and inhibition, (2) structural or textural aging, (3) coking and fouling, (4) sintering and recrystallization, (5) attrition and crushing, and (6) loss of the active phase due to volatilization.[1,5,6] These causes can often be inter-correlated; for example, sulphur can simultaneously cause poisoning and sintering of noble metals due to strong chemical adsorption and increased mobility at high temperatures. The literature on industrial catalyst deactivation is limited, typically focusing on one or two catalyst systems, and often relies on *ex situ* analysis rather than studying catalysts in relevant environments (*e.g.*, under specific atmospheres, temperatures, and pressures). The deactivation of CuZnO catalysts, particularly in industrial applications, is a complex issue that spans from micro to macro scales. These catalysts are widely used in processes like methanol steam reforming (MSR), water–gas shift (WGS), and hydrogenation reactions due to their excellent activity at low temperatures.[7–9] ZnO is well known to volatilize under reducing temperatures higher than 500 °C, causing significant restructuring and crystallization of the active phase.[10] However, the stability of ZnO within mixed metal oxides at lower temperatures, *e.g.*, 160–240 °C is less understood. A recent study by Redekop *et al.* investigated the stability of Zn within a $ZnZr_2O_4$ matrix under reducing conditions across a wide temperature range.[7] This study revealed that Zn can volatilize from ZnO at elevated temperatures ($T > 550$ °C) leading to catalyst deactivation and reduced selectivity. Additionally, the mobility of Zn within the catalyst structure is also significant, with zinc species able to move between the solid solution phase with ZrO_2 and segregated ZnO clusters. This mobility is partially reversible under reductive heat treatment above 250 °C.[7] Several studies have investigated the structural and electronic changes in Zn and Cu within a $CuZnO/Al_2O_3$ catalyst under both reducing and oxidizing conditions.[8,9,11] Using *operando* spectroscopy, it has been shown that CuZn alloys are formed depending on the partial pressure of hydrogen and temperatures. However, these studies have not explored the mobility of Zn species and the potential implications for catalyst stability.

This research sought to understand the failure mode of co-precipitated CuZnO-based materials under industrial hydrogenation conditions. Prior to discharging the reactor bed, the spent catalyst undergoes an oxidation treatment for safety reasons. As a result, post-mortem characterization and data interpretation need to be performed carefully, since this treatment can further introduce changes in the structure and composition of the material. Through careful interpretation of microscopy analysis results, we identified characteristic fingerprints of the failure mechanisms. These insights can be leveraged to develop more stable hydrogenation catalysts.

Results and discussion

Fig. 1 illustrates an example of the catalyst deactivation of CuZnO-based catalysts during a mild hydrogenation process (160–240 °C). In this case, catalyst deactivation is characterized by an increase in the pressure drop from the middle of the reactor of a downflow adiabatic reactor. The rapid increase in the pressure drop is highly undesirable since it limits production, causing process shutdowns and catalyst replacements.[12] In some industrial applications, the physical breakage (or loss of crush strength) of catalyst pellets is the primary cause of process shutdowns instead of the loss of activity and selectivity. The effect of the mechanical failure of catalyst pellets on the pressure drop has been examined by Wu *et al.*[12] The results revealed that along with the mechanical failure of the pellets there exists a point of maximum curvature around which the rate of the pressure drop increases very rapidly. This acceleration in the pressure drop was attributed to a mutation of the packing structure, as the failed pellets reach a certain critical threshold. Above that critical threshold, the rapid increase in the pressure drop does not result from the rapid increase of the amount of broken particles or fines, but from changes in the pellet packing density. In this case, the change in the catalyst pellet packing density was also evident by the significant change in bed porosity (void fraction estimated by the Ergun equation) and consequently shrinkage of the catalyst bed relative to the initial catalyst volume; it is

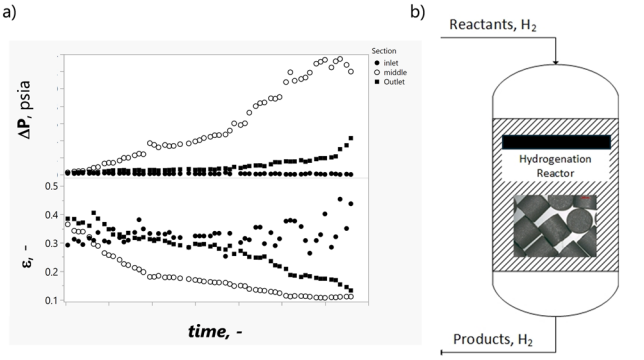

Fig. 1 a) Evolution of the pressure drop (ΔP) and void fraction (ε) of the catalyst bed as a function of age for the inlet, middle and outlet sections. b) Representation of the downflow adiabatic hydrogenation reactor with the correspondent inlet and outlet temperatures. The pressure drop is measured using pressure sensors across different positions of the catalyst bed. Before and after the run, the catalyst bed height is measured using tape measurements to assess the bed shrinkage. The bed shrinkage was ~15–20%.

estimated around 20% decrease in the catalyst bed volume which is consistent with the experimental estimated value, suggesting a change in bed porosity and the packing structure. Understanding the root cause for the loss of the mechanical integrity of the CuZnO catalyst pellets during a mild hydrogenation process is crucial for extending the catalyst's lifetime.

Catalyst pellets from different positions in the reactor were studied using various analytical characterization techniques and compared with a fresh batch material. Low-magnification stereo-microscopy analysis was conducted to visually inspect modifications in the pellet shape, as shown in Fig. 2. The fresh pellets are uniformly cylindrical, while the spent pellets exhibit significant deformation and degradation. Differences in pellet alterations were found at different positions in the reactor bed. The pellets from the inlet (top) were rounded, while the pellets from the middle section showed plastic deformation under mechanical stress. Pellets near the bottom of the reactor showed significant fracturing. Although the stereo micrographs show clear dependence on the reactor bed position, analyses by scanning electron microscopy (SEM) showed variations in crystallite sizes, morphologies, and voids for pellets throughout the entire catalyst bed. As shown in Fig. 3, the fresh catalyst exhibited a uniform morphology with very small crystals, while the spent catalysts showed notable local crystal growth. Crystals ranging from 20 to 200 nm in size were observed, and energy-dispersive X-ray (EDX) analysis confirmed that these crystals correspond to the ZnO phase. The coarsening of crystallites from the nanometer to micron size significantly reduces the interparticle cohesion and increases pore sizes in the pellet structure. As a result, the pills are weakened making them vulnerable to erosion, deformation, and fracture under the gravitational load. The structural changes of the catalyst pellets increase the packing density in the reactor and cause an increase of the reactor pressure drop aging slope (see Fig. 1). The long-range crystalline order of the fresh and spent CuZnO-based catalysts, taken from the inlet, middle, and outlet sections of the reactor, was investigated using X-ray diffraction (XRD). Fig. S1† presents the estimated crystal domain size of ZnO and CuO, determined by the Scherrer equation, for spent catalysts. These analyses indicate growth in the crystal domain size of ZnO from 11 to 25 nm. XRD measured the average crystal growth and therefore cannot be directly compared with SEM, which clearly indicates local crystal growth varying from 20–200 nm. The CuO crystal domain also increased slightly from 8 to 10 nm.

ZnO is a key component in the Cu-based mixed oxide catalyst used for hydrogenation reactions and is known to volatilize under high-temperature conditions.[10] However, very little is known about the mobility and volatility of ZnO within CuZnO mixed oxides under mild hydrogenation conditions. Since the restructuring/volatilization of ZnO are highly dependent on the type of mixed metal oxide, synthesis conditions, and gas phase atmosphere, a systematic study was conducted on CuZnO-based catalysts to understand the stability of ZnO upon exposure to H_2 treatment and to determine if this is the root cause for the pressure drop increase with age. These experiments were crucial to evaluate whether ZnO sintering is likely under mild hydrogenation conditions or if an impurity in the feed is accelerating the ZnO sintering.

Stereomicroscopy, SEM, XRD, and XPS analyses were conducted before and after a reduction treatment at 270 °C for one week to assess the potential impact of reducing conditions on ZnO sintering and the mechanical stability of the pellets. This experiment used a significantly higher reduction temperature (270 °C) compared to the hydrogenation process to accelerate potential ZnO sintering. Fig. 4 shows the SEM images of fresh and reduced pellets. Microscopy indicates no significant change in the catalyst's morphology, although some crystal size coarsening was observed, after reduction. XRD analysis on hydrogen-treated materials exhibited sharper and more intense diffraction peaks of the ZnO phase (Fig. S2†), consistent with an increase in the crystallite size and crystallinity, as observed by SEM. Although these experiments demonstrated some coarsening of ZnO under reducing conditions, they could

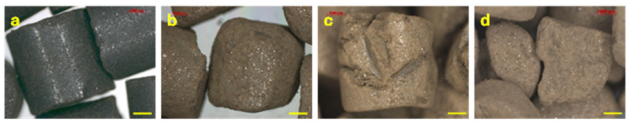

Fig. 2 Stereomicrographs of the (a) fresh, (b) spent inlet, (c) middle and (d) outlet. Scale bar is 1000 μm.

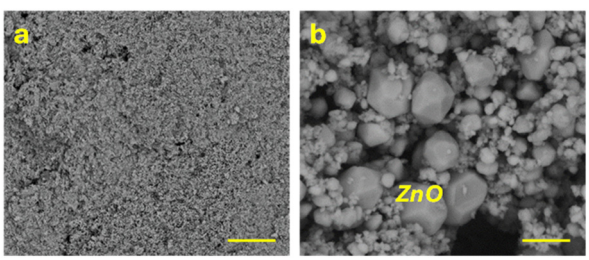

Fig. 3 SEM micrographs of the pellet cross section of the a) fresh and b) spent CuZnO-based catalyst. The scale bar is 500 nm.

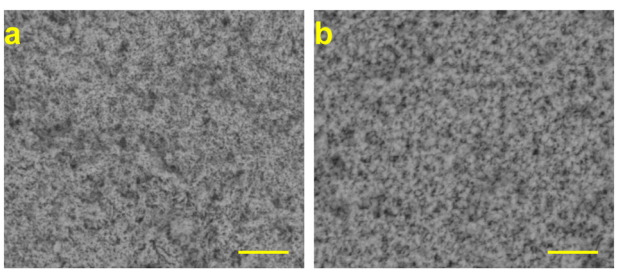

Fig. 4 SEM micrographs of the (a) fresh and (b) reduced CuZnO catalyst. Reduction treatment was done at 270 °C under 10% H_2/inert for 7 days. Scale bar is 500 nm.

not replicate the local ZnO crystal growth and crystallization that may lead to a loss of crush strength. One leading hypothesis for the increased pressure drop during operation is that impurities in the feed promoted the sintering and crystallization of the ZnO component resulting in pellet weakening, shape degradation, and differences in reactor bed packing. To test this hypothesis, trace compositional analysis (XRF) was performed on the spent catalysts and fines to identify potential impurities. XRF analysis, summarized in the ESI,† revealed substantial amounts of chloride on the catalyst (up to 1000 ppm). Chloride is a known poison for CuZnO-based systems, since it can react with Cu and ZnO components to form surface CuCl and $ZnCl_2$ species.[5] However, previous studies have focused on the loss of Cu activity rather than the structural changes caused by chloride impurities. It is well known that, compared to metal oxides, metal chlorides are lower-melting and have lower surface energies (see thermochemical analysis in the Fig. S7†), due to differences in the bond strengths and the structural nature of the chemical bonding.

For example, Tammann and Hüttig temperatures can be used to estimate the surface and bulk mobility and directly correlated with the sintering rate ability (see Fig. S7†). This analysis points to high mobility for the metal chlorides; for example, $ZnCl_2$ is very mobile at 200 °C, while ZnO is only mobile at temperatures above ~700 °C. As a result, chloride impurities can accelerate the sintering that leads to the weakening of the catalyst pellets, and subsequent early termination of the useful life of the catalyst. In addition, chloride is likely to be enriched at surfaces and grain boundaries, further weakening the interfacial cohesion that binds the crystallites together into the particles that make up the catalyst pills. In summary, chloride impurities are likely to accelerate the weakening of the catalyst pills, leading to structural modifications of the catalyst pills, *e.g.*, erosion, deformation, and fracture, and a subsequent increase in the reactor pressure drop. To test this hypothesis, an accelerated aging study was performed with ethyl chloride and hydrogen in the feed.

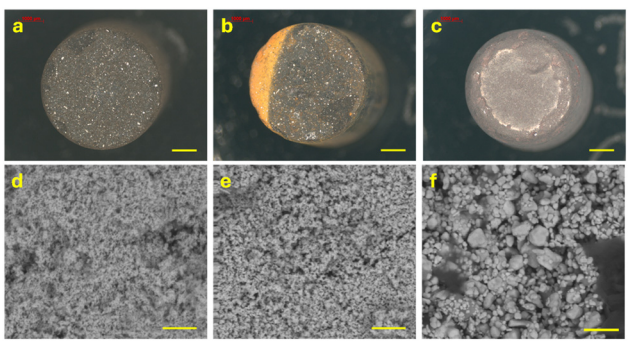

Fig. 5 Stereomicroscopy (top) and SEM images (bottom) showing catalyst structure evolution from (a and d) fresh to (b and e) H_2 treatment and (c and f) after Cl-treatment. Micrographs were acquired on the pellet top surface. The scale bar is 1000 μm (top) and 500 nm (bottom). Elemental maps of K (red) and Zn (blue) for (d) fresh and (e) H_2 treatment, and (f) K (red) and Cl (green) distribution after aging with Cl. The scale bar is 200 μm. Elemental maps of K (red) and Zn (blue) for (d) fresh and (e) H_2 treatment, and (f) K (red) and Cl (green) distribution after aging with Cl. The scale bar is 200 μm.

This experiment was conducted under the same conditions as the reducing treatment, but with the addition of 10 ppmv of ethyl chloride in the gas phase. The SEM and stereomicroscopy images of chloride-treated catalysts are shown in Fig. 5, S4–S6,† and as relative comparison, the spent catalysts taken from the outlet of the reactor are also included. The chloride treatment caused significant local ZnO crystal growth from 15 to ~20 nm (see the Fig. S3†). Furthermore, the morphological and structural changes observed in chloride-aged catalysts and in spent catalysts with a reduced lifetime are remarkably similar, suggesting that this treatment successfully reproduced the failure mode observed during the hydrogenation reaction. EDX mapping of chloride-treated samples (Fig. S5†) showed that chloride is present within the pellet, with an enrichment on the surface.

Additional X-ray diffraction (XRD) analysis was done on chloride-treated catalysts to quantify changes in the crystalline structure and crystal domain size. Fig. S2† shows the diffraction patterns before and after chloride treatments. For comparison, reference compounds such as ZnO and CuO are also included. The quantification of each crystalline phase and crystal domain size was obtained using a whole pattern fitting procedure (the Easy-Quant module of the Jade 9.5 software package). After chloride treatment, there was a substantial increase in the intensities and sharpening of the peaks corresponding to ZnO and metallic Cu, indicating a further increase in the crystal domain size. No oxidized Cu species were found after the chloride treatment, which could be due to the formation of larger crystals, reducing the rate of metal re-oxidation upon contact with air.

Chloride treatment increased the average crystal domain size from 15 to 19 nm. These studies demonstrate the catastrophic effect of chloride impurities on the structural and mechanical properties of CuZnO pellets besides the effects described in the literature related to the loss of catalyst activity and selectivity.[5] The reaction of ZnO with chloride creates the precursors for sintering, leading to local crystallisation, and the formation of voids that affect substantially the crush strength of the resultant materials. Developing more robust catalysts to chloride impurities is highly desirable for hydrogenation processes.

Conclusions

Unexpected catalyst failures can have significant economic impacts on plant operations. This study exemplifies how the application of post-mortem analysis at different length scales and development of accelerating aging tools can be used to understand a catalyst failure mode on CuZnO-based catalysts at the industrial scale. Careful interpretation of the results from microscopy analysis enabled the identification of characteristic fingerprints of the failure mechanism. Under reducing conditions, CuZnO-based catalysts are very sensitive

to the presence of chloride in the feed. ZnO reacts with chloride in the feed forming the precursors for sintering causing substantial ZnO local crystal growth, giving a premature loss of the useful catalyst life due to the erosion and deformation of the catalyst pills and a concomitant excessive reactor pressure drop. Understanding these mechanisms at both micro and macro scales is crucial for developing more durable and efficient CuZnO catalysts for industrial applications.

Experimental

Catalyst

The catalysts used in this study are bulk CuZnO-based catalysts synthesized by co-precipitation as described herein.[13] A series of fresh and aged catalysts representative of short and long catalyst lifetimes were characterized by SEM and XRF.

Aging experiments

The aging experiments were carried out under a controlled atmosphere for 1 week at 270 °C and 1 bar with a feed containing 10% H_2, 10 ppmv ethyl chloride and inert (nitrogen). For relative comparison, a baseline experiment was done under the same temperature, pressure and duration in the presence of 10% H_2/inert (no ethyl chloride) to assess thermal aging effects. These experiments were carried out in a Symyx HIP/SOSS System that is designed to mix *via* orbital shaking the gas/solid contents of a reactor vessel under a common headspace, pressure, and temperature. The HiP/SOSS System consists of a Single Reactor SOSS System (Single-Heated Orbital Shaking System), "Super" HiP reactors, reactor inserts with pinhole plates and gaskets and a feed system (back pressure controller, 3xMFC). Each shaker has temperature and orbital speed control. Control is either manual or remote *via* RS232 communication. Gas supply flow rate is controlled using a computer. Each reactor can accommodate 24 samples. In a typical experiment, 250 mg of catalysts in pellet (up to 3 pellets) or powder (60–80 mesh) form are loaded in the reactors. Prior to the aging process, the catalysts were heated from room temperature to 220 °C under an inert atmosphere using a heating rate of 5 °C min^{-1}, followed by a reduction under 10% H_2/N_2 for 2 hours at the same temperature. After reduction, the catalysts were subsequently heated to 270 °C using a heating rate of 5 °C min^{-1}, and exposed to a gas mixture containing 10% H_2, 10 ppmv ethyl chloride and nitrogen (balance). The catalysts were aged under these conditions for one week. The conditions selected for this test aimed to accelerate the aging process. Ethyl chloride was selected for the aging studies since the preliminary analysis of the hydrogen feed demonstrated the presence of small amounts of methyl chloride (<15 ppb).

Stereomicroscopy

Images of catalyst pellets were acquired on a Stereo Light Microscope Stemi 2000-C Zeiss in reflected mode using AxioCam ICc1 with AxioVision 4.8 image software.

Scanning electron microscopy (SEM)

The SEM images were obtained with a NOVA nanoSEM 600 (FEI, Eindhoven, The Netherlands) operated using immersion mode at low vacuum (40 Pa) with an accelerated voltage of 3 kV and spot 4. The SEM images were recorded using a GAD backscattered electron detector.

Energy-dispersive X-ray spectroscopy (SEM-EDX)

EDX spectra were acquired using an X Flash detector 4030 (BRUKER AXS) using SEM operating conditions of 5 kV and spot 6 or 20 kV and spot 5.5.

X-ray photoelectron spectroscopy (XPS)

X-ray photoelectron spectroscopy (XPS) was used to analyse the surface chemistry of the side of each catalyst sample and the cut and uncut ends of some samples. This gives an indication of the effect of exposure to chlorine on the elemental composition of the catalyst surface. The samples were provided as cylinders that had a diameter of approximately 5 mm and a length of approximately 5 mm. It was decided to analyse the surface of the side of each sample and the circular end of the sample. A razor blade was used to cut the cylinder to reduce the height to approximately 2 mm.

XPS analysis was performed using an Axis Ultra spectrometer (Kratos Analytical). Samples were irradiated with monochromated X-rays (Al Kα, 1486.6 eV) with photoelectrons analysed from a selected area 700 micron by 300 micron, with a take-off-angle of 90°. Each analysis position was analysed in the survey mode (pass energy 160 eV) to determine the elements that were present at the surface and their relative concentrations. CasaXPS (Casa Software Ltd) data processing software was used to calculate the area under peaks representative of elements detected, which were then normalized to take into account relative sensitivity to provide relative concentrations. Each analysis position was also analysed in the high-resolution mode (pass energy 20 eV) to determine more detailed information on the elements present at the surface. Charge correction was conducted using a method of the internal standard. Peaks representative of the known chemical states were fitted to high-resolution core level spectra. The measured binding energy of these peaks (BE_{meas}) was used with a relevant reference binding energy (BE_{Ref}) with CasaXPS (Casa Software Ltd) data processing software to apply a correction energy, Δ_{corr} to all the spectra acquired from the same analysis position.

X-ray powder diffraction (XRPD)

Fine powders of catalytic materials were carefully transferred onto a silicon sample holder (a few mg). The XRPD analyses were carried out under ambient lab conditions on a Bruker AXS diffractometer D8 Discover with a general area diffraction detector system (GADDS) using Cu Kα (λ = 1.5406 Å) with 2 theta ranges from 9–70° and with a 0.05°

integration step size. The XRPD patterns, after 2 theta calibration against a reference standard (Al_2O_3 corundum, PDF# 00-046-1212). The analyses were carried out using the 'JADE 9.5 Plus XRD Pattern Processing, Identification & Quantification' program (Materials Data, Inc. 1995–2013), which uses the International Centre for Diffraction Data (ICDD) database of XRD patterns to identify the crystalline phase(s) observed in the XRPD patterns. The JADE version (basic version of the jadewpf module) gives semi-quantitative estimates of the primary crystallite sizes.

X-ray fluorescence

X-ray fluorescence (XRF) data were collected at room temperature (RT) with a PANalytical PW4400 spectrometer using an X-ray tube with a rhodium anode.

Process modelling

Mass balance, energy balance, and Ergun equations of a standard adiabatic reactor are solved along the length of the reactor. The model results are compared with the measured temperature and pressure profiles inside the reactor to estimate the activity and void fraction of the catalyst bed in each section of the bed.

Data availability

The data supporting this article have been included as part of the ESI.†

Author contributions

All authors contributed equally to writing the paper.

Conflicts of interest

There are no conflicts of interests.

Acknowledgements

The authors acknowledge Ailene Phillips and Patrick Heider, for helpful discussions.

References

1 J. A. Moulijn, A. E. Diepen and F. Kapteijn, Catalyst Deactivation: Is It Predictable? What to Do?, *Appl. Catal., A*, 2001, **212**, 3–16.
2 E. Filippi and C. Pizzolitto, The Past and the Future of Catalysis and Technology in Industry: A Perspective from Casale SA Point of View, *Catal. Today*, 2022, **387**, 9–11.
3 A. J. Martín, S. Mitchell, C. Mondelli, S. Jaydev and J. Pérez-Ramírez, Unifying Views on Catalyst Deactivation, *Nat. Catal.*, 2022, **5**, 854–866.
4 V. P. Santos, E. Tocha, J. Yang, M. McAdon, C. Schmidt, S. Leadley, D. Yancey, S. van Bloois, J. Depicker, S. Naik, L. Bui, S. Bhandari, D. Grohol and D. G. Barton, *Fundamentals of Industrial Problem Solving*, ed. W. Medlin, 2022.
5 H. Huang, S. Wang, S. Wang and G. Cao, Deactivation Mechanism of Cu/Zn Catalyst Poisoned by Organic Chlorides in Hydrogenation of Fatty Methyl Ester to Fatty Alcohol, *Catal. Lett.*, 2010, **134**, 351–357.
6 A. J. Martín, S. Mitchell, C. Mondelli, S. Jaydev and J. Pérez-Ramírez, Unifying Views on Catalyst Deactivation, *Nat. Catal.*, 2022, **5**, 854–866.
7 E. A. Redekop, T. Cordero-Lanzac, D. Salusso, A. Pokle, S. Oien-Odegaard, M. F. Sunding, S. Diplas, C. Negri, E. Borfecchia, S. Bordiga and U. Olsbye, Zn Redistribution and Volatility in ZnZrO x Catalysts for CO2 Hydrogenation, *Chem. Mater.*, 2023, **35**, 10434–10445.
8 A. Beck, M. Zabilskiy, M. A. Newton, O. Safonova, M. G. Willinger and J. A. van Bokhoven, Following the Structure of Copper-Zinc-Alumina across the Pressure Gap in Carbon Dioxide Hydrogenation, *Nat. Catal.*, 2021, **4**, 488–497.
9 M. Zabilskiy, V. L. Sushkevich, D. Palagin, M. A. Newton, F. Krumeich and J. A. van Bokhoven, The Unique Interplay between Copper and Zinc during Catalytic Carbon Dioxide Hydrogenation to Methanol, *Nat. Commun.*, 2020, **11**, 2409.
10 D. F. Anthrop and A. W. Searcy, Sublimation and Thermodynamic Properties of Zinc Oxide, *J. Phys. Chem.*, 1964, **68**, 2335–2342.
11 A. Beck, M. A. Newton, M. Zabilskiy, P. Rzepka, M. G. Willinger and J. A. van Bokhoven, Drastic Events and Gradual Change Define the Structure of an Active Copper-Zinc-Alumina Catalyst for Methanol Synthesis, *Angew. Chem., Int. Ed.*, 2022, **61**, e202200301.
12 D. Wu, L. Song, B. Zhang and Y. Li, Effect of the Mechanical Failure of Catalyst Pellets on the Pressure Drop of a Reactor, *Chem. Eng. Sci.*, 2003, **58**, 3995–4004.
13 S. Fujita, S. Moribe, Y. Kanamori, M. Kakudate and N. Takezawa, Preparation of a Coprecipitated Cu/ZnO Catalyst for the Methanol Synthesis from CO2 — Effects of the Calcination and Reduction Conditions on the Catalytic Performance, *Catal. Sci. Technol.*, 2001, **207**, 121–128.